

*2.3.b. Assumptions Related to the PED in Figure 5a and
the TD of the Uranian Protosatellite Disk*

The observations in the last section cause us to explore the possibility that the PED in Fig. 5a is related to the TD of the Uranian protosatellite disk. To do this we first make a series of simplifying assumptions: 1. The present day orbital radii of the Uranian satellites and rings (R_u) are the same or nearly the same as the orbital radii of the primordial rings from which they evolved. If migration does affect Uranian satellite orbital radii, the migration is uniform for all the satellites. 2. The Uranian rings and regular satellites evolved from primordial rings that were born in the Uranian protosatellite disk. 3. Each primordial ring is associated with the local mid-plane temperature of the disk. 4. Each of these T 's is related to a photon energy (E_p) in the portion of the H_2 spectrum in Table 4. 5. The relationship between T and E_p is linear and of the form

$$T = C_1(E_p + C_2), \quad (3)$$

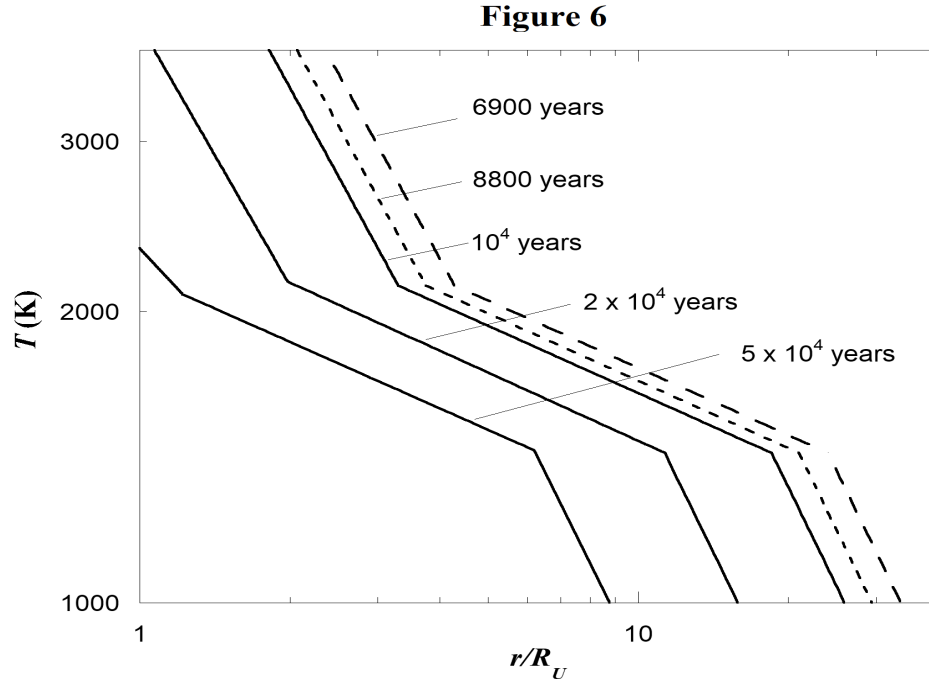
where C_1 and C_2 are constants empirically determined in section 2.3.c.

Section 2.6 and Appendix 3 theoretically link E_p 's to specific disk temperatures (T 's) in the linear form of Eq. (3).

2.3.c Determination of C_1 and C_2

Mousis (2004) derives a series of TD's for a "water-rich" Uranian protosatellite disk. Each TD is for a different time t after the disk is formed by an assumed impact to Uranus's surface. Fig. 1 of Mousis (2004) has seven TD's with t values for the first three equal to 1×10^4 , 2×10^4 and 5×10^4 years. Fig. 6 in

**Fig. 6. TD's with solid lines: Mousis (2004)
TD's with dashed lines: present investigation**



the present investigation includes reproductions of the first three Mousis TD's (each represented by solid straight line segments) and two TD's (dashed line segments) constructed in the present investigation by using the similarities among the first three Mousis TD's. Appendix 1 is a discussion of the method used for the reproduction of the Mousis TD's and for the construction of the two dashed TD's. The t values for TD's are indicated in Fig. 6. Three of these are from Mousis (2004) and the other two associated with the dashed TD's are $t = 8800$ and 6900 years. A discussion of how these two t 's are determined is in Appendix 2.

Table 4 and the time dependent series of TD's in Fig. 6 are used to determine the parameters C_1 and C_2 in Eq. (3). Because graphs in Fig. 6 do not contain a dip and a peak as is seen in the Uranian PED in Fig. 5a, the only E_p 's and R_{ui} 's used in the process are those in the PED's "tail" for which $i = 9 - 20$ in page 2 of Table 4. This parameters are found as follows. Many trial sets of C_1 and C_2 are used in Eq. (3). For each set of C_1 and C_2 , a set of T 's is calculated with each T in a set corresponding to an E_p and a R_{ui} in Table 4. Then each set of T 's and R_{ui} 's is graphed to make a trial TD and the trail TD is compared to the TD's in Fig. 6.

Best fits to the Mousis (2004) TD's for which $t = 1 \times 10^4$, 2×10^4 and 5×10^4 years are found and the best of the three is the one for the earliest time $t = 1 \times 10^4$ years shown in Fig. 7. But it is seen that a Mousis type TD for an earlier time would most likely be fitted even better. Various earlier time Mousis type TD's are constructed using a method discussed in Appendix 1. By trial and error it is found that the TD corresponding to $t = 8800$ years is fitted best of all. This TD and the fitted data are given in Fig. 8. The corresponding parameters are $C_1 = 2.315 \text{ K} \cdot \text{cm}$ and $C_2 = -3720 \text{ cm}^{-1}$. The time $t = t_0 = 8800$ years is the approximate time when the Uranian satellites start their formation. The best fit to the TD for $t = 6900$ years is given in Fig. 9. It is interesting to compare Figs. 7, 8 and 9. The times $t_0 = 8800$ and 6900 years are determined in Appendix 2.

Fig. 7. Line segments: The TD for $t = 1 \times 10^4$ years (Mousis (2004)).
The point wise TD is determined by varying C_1 and C_2 in Eqn. (3).

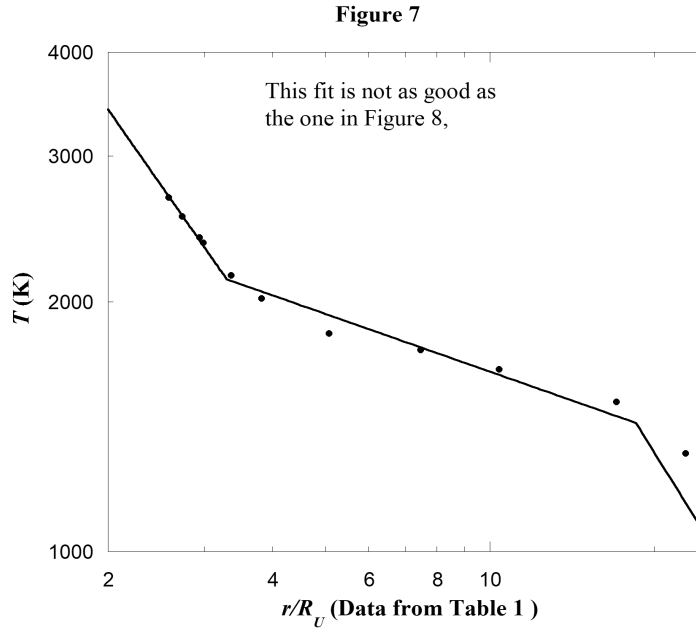


Fig. 8. Line segments: The Mousis "type" TD for $t = t_0 = 8800$ years.
The point wise TD is determined by varying C_1 and C_2 in Eqn. (3).

Figure 8

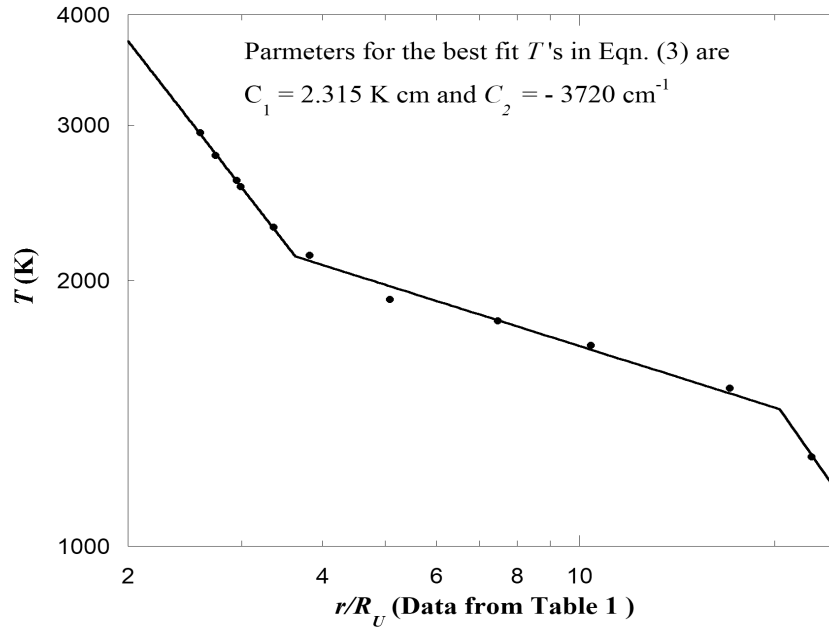
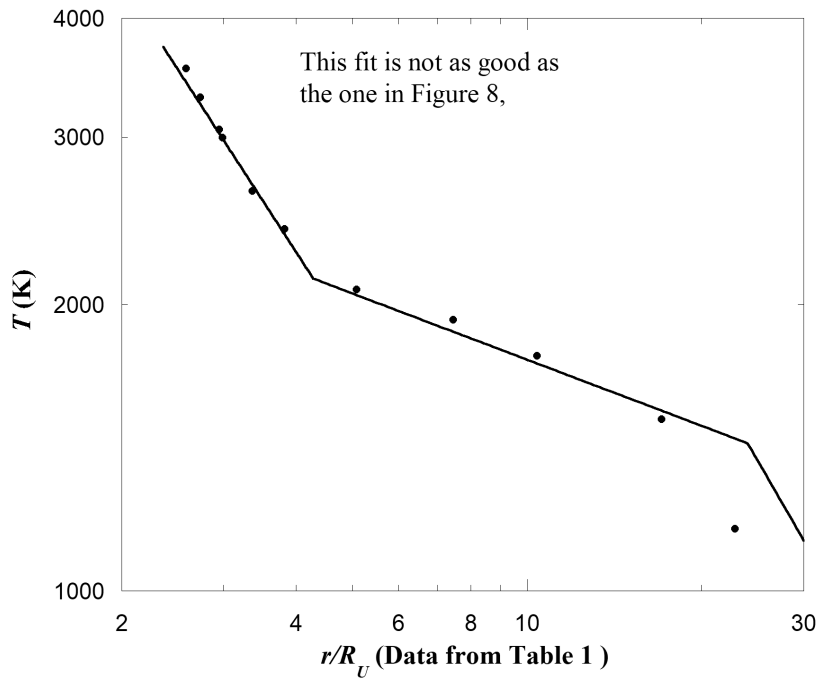


Fig. 9. Line segments: The Mousis "type" TD for $t = t_0 = 6900$ years.
The point wise TD is determined by varying C_1 and C_2 in Eqn. (3).

Figure 9

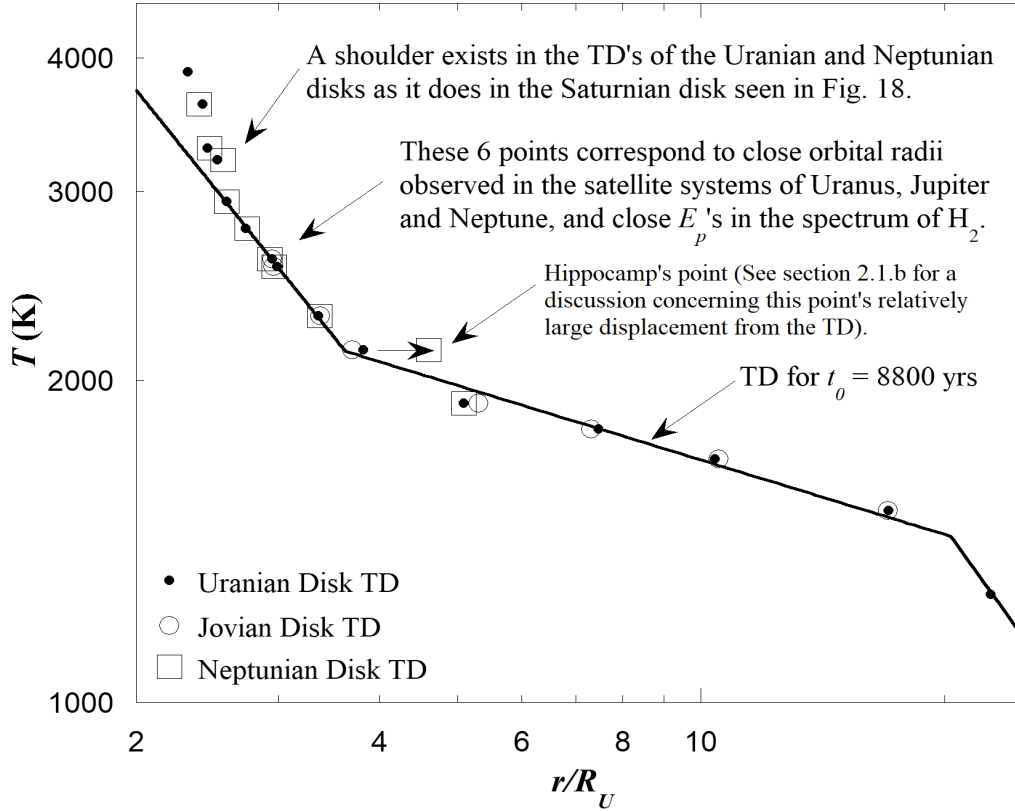


2.4. The Overlap of the Uranian, Jovian and Neptunian TD's

Table 2 contains transformed orbital radii of the Jovian and Neptunian satellites. It is used in section 2.1.c to construct Fig. 3. Now we use it again to construct the scaled Jovian and Neptunian TD's seen in Fig. 10. This figure also includes the graphs shown in Fig. 8 for the Uranian TD for which $t = t_0 = 8800$ years. Fig. 10 shows the generally precise overlap of the three TD's. As discussed in section 2.1.c, this overlap cannot continue inward to smaller orbital radii because the Jovian and Neptunian protosatellite disks are relatively closer to their respective planets than is the Uranian disk from Uranus. Interestingly, in the upper left the shape of the Uranian and Neptunian TD's both show a “shoulder”. In a future discussion we see a similar shoulder in Saturn's TD.

Fig. 10. Radial scaling causes the Uranian, Jovian and Neptunian TD's to overlap.

Figure 10



In the present model Uranian satellites begin their formation 8800 years after the the Uranian protosatellite disk was formed. Because the Jovian and Neptunian TD's overlap the Uranian TD for which $t = 8800$ years, we may think it is possible to draw conclusions about the times when the Jovian and Uranian satellites begin their formation. But this is not true. For the most part, TD's corresponding to different times in the vicinity of $t = 10^4$ years can be transformed from one to another simply by linearly scaling the radial coordinate system associated with one of them. So Eqs. (1) and (2) scale TD's with respect to both time and space but we don't know to what degree for each.

Table 5. Photon energies (E_p 's) are used to calculate the Uranian protosatellite disk temperatures (T 's). The T 's and orbital radii (R_u 's) are used to construct the complete Uranian TD in Fig.11. All T 's are calculated from Eq. (3) with $C_1 = 2.315\text{K}\cdot\text{cm}$ and $C_2 = -3720\text{ cm}^{-1}$.

Satellite	i	$E_p(\text{cm}^{-1})^a$	$T(K)$	R_u^b
Ring 6	11&12	4826	2560	1.637
Ring 5	13&14	4712	2296	1.652
Ring 4	15	4642	2134	1.666
Ring α	15	4642	2134	1.750
Ring β	13&14	4712	2296	1.786
Ring η	11&12	4826	2560	1.846
Ring γ	10	4917	2771	1.863
Ring δ	9	4990	2939	1.900
Cordelia	7	5108	3213	1.948
Ring λ	5&6	5144	3296	1.957
Ring ϵ	3&4	5285	3623	2.006
Ophelia	1	5397	3882	2.105
Bianca	1	5397	3882	2.316
Cressida	3&4	5285	3623	2.418
Desdemona	5&6	5144	3296	2.453
Juliet	7	5108	3213	2.520
Portia	9	4990	2939	2.586
Rosalind	10	4917	2771	2.735
Cupid				2.911
Belinda	11	4841	2596	2.946
Perdita	12	4823	2553	2.990
Puck	13&14	4712	2296	3.365
Mab	15	4642	2134	3.824
Miranda	16	4543	1904	5.082
Ariel	17	4498	1800	7.469
Umbriel	18	4449	1688	10.410
Titania	19	4372	1510	17.070
Oberon	20	4265	1262	22.830

^aBlack van Dishoeck (1987). Some E_p 's are weighted averages.

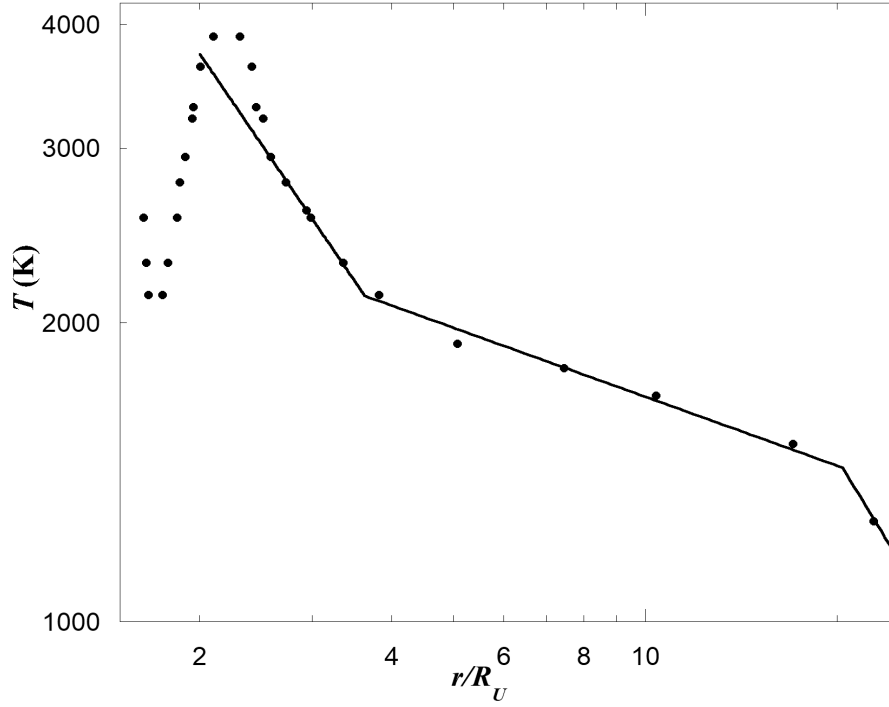
^bNASA (2021)

2.5. The Complete TD for the Uranian Protosatellite Disk

Eq. (3) relates T 's to E_p 's. The constants in this relationship are determined in section 2.3.c by fitting data to the “tail” of the Uranian disk TD. We now assume Eq. (3) holds for the complete Uranian disk TD. Table 5 lists the complete set of calculated T 's, and Fig. 11 shows the complete point-wise TD. Because the relationship between T and E_p in Eq. (3) is linear, the Uranian TD and PED have similar shapes. Therefore the Uranian disk TD also shows characteristics described by L&P (1985) for the solar nebula as described in section 2.3.a. Notice the present investigation diverges from the Mousis “type” graph at a point just to the right of the peak. A similar result is seen later in Fig. 18 where Saturn TD's are compared.

Fig. 11. The complete Uranian disk TD overlapping the Mousis (2004) “type” TD ($t = t_0 = 8800$ years)

Figure 11



2.6. Why are T and E_p related in the Form Given by Eq. (3)?

Stancil and Dalgarno (1997) have used the mechanism of SRMA to study rate coefficients for the production of the molecule LiH from the atoms Li and H in the early universe. The form of the reaction describing SRMA is



where A and B are atoms or molecules that associate to make the molecule AB . The photon $h\nu$ on the left side of Eq. (4) stimulates the process during which a second photon is created with the same energy and direction of motion as the first. And so there are two photons symbolized on the right side.